Proceedings of the ASME 2009 Heat Transfer Summer Conference
HT2009
July 19-23, 2009, San Francisco, California USA

HT2009-88607

NATURAL CONVECTION HEAT TRANSFER FROM VERTICAL TRIANGULAR DUCTS.

Mohamed E. Ali and Hany Al-Ansary
King Saud University, College of Engineering, Mechanical Engineering Department,
P. O. Box 800, Riyadh 11421, Saudi Arabia.
Phone : +966-1-467-6672, Fax : +966-1-467-6652, E:mali@ksu.edu.sa, hansary@ksu.edu.sa

ABSTRACT- Experimental investigations have been reported on steady state natural convection from the outer surface of vertical triangular cross section ducts in air. Three ducts have been used with equilateral side length of 0.044, 0.06 and 0.08 m. The ducts are heated using internal constant heat flux heating elements. The temperatures along the vertical surface and the peripheral directions of the duct wall are measured. Axial (perimeter averaged) heat transfer coefficients along the side of each duct are obtained for laminar and transition to turbulent regimes of natural convection heat transfer. Axial (perimeter averaged) Nusselt numbers are evaluated and correlated using the modified Rayleigh numbers for laminar and transition regime using the vertical axial distance as a characteristic length. Critical values of the modified Rayleigh numbers are obtained for transition to turbulent. Furthermore, total overall averaged Nusselt numbers are correlated with the modified Rayleigh numbers for all ducts. The local axial (perimeter averaged) heat transfer coefficients are observed to decrease in the laminar region and increase in the transition region. Laminar regimes are obtained at the lower half of the ducts and its chance to appear decreases as the heat flux increases.

Keywords: Natural convection, triangular ducts, experimental heat transfer, laminar and transition regimes.

1- INTRODUCTION

Steady state natural convection from vertical triangular cross section ducts has many engineering applications in cooling of electronic components, design of solar collectors and heat exchangers. Vliet and Liu [1] have proposed the following local correlation for turbulent natural convection from a vertical flat plate in water subjected to constant heat flux.

$$Nu_x = 0.59 \left(Ra_x^*\right)^{0.22}, 1.0x10^{13} \le Ra_x^* \le 1.0x10^{16} \qquad (1)$$

They have defined laminar and transition to turbulent based on decreasing or increasing in the local plate surface temperature differences respectively which corresponding to increasing or decreasing in the local heat transfer coefficient. Churchil and Chu [2] have suggested a correlation for the average Nusselt number from a vertical plate over the entire range of Rayleigh number using the plate height as a characteristic length. Their equation is cited here for comparison.

$$\overline{Nu} = \left[0.825 + \frac{0.387\,Ra^{1/6}}{\left[1+(0.437/Pr)^{9/16}\right]^{8/27}}\right]^2 \qquad (2)$$

Natural convective heat transfer from a short isothermal cuboid has been studied analytically and experimentally in air by Radziemska and Lewandowski [3]. On the other hand, Kimura et al. [4] have investigated the natural convective flows of water induced around heated vertical cylinders. In their results they observed that, the local heat transfer coefficients have their highest value at the leading edge. Furthermore, they decrease gradually with the distance away from the leading edge up to a minimum value at some distance downstream and then they turn to increase up to a constant value. Experiments on laminar free convective heat transfer from sidewalls of a vertical square cylinders in air have reported by popiel and wojtkowiak [4] using a lumped capacitance method. Their results were 9-12% higher then the data of Churchill and Chu [2] for isothermal flat plate. Furthermore, a theoretical investigation is carried out by Gori et al [5] to study natural convection around a vertical thin cylinder or needle heated at uniform and constant wall heat flux using the local non-similarity method. Recently, Popiel et al. [6] have presented an experimental study of the laminar free convective average heat transfer in air from isothermal vertical slender cylinder using a transient technique. Moreover, correlations for natural convection heat transfer from helical coils were reported by Ali [7-10] for different Prandtl numbers in laminar and turbulent regimes. Recently, Ali [11] has reported experimental free convection study for horizontal rectangular and square ducts in air. In his study; empirical correlations are reported for local and average heat transfer for both laminar and transition regimes around the ducts. On the other hand, Zeitoun and Ali [12] have reported

numerical simulations of natural convection heat transfer from isothermal horizontal rectangular cross section ducts in air. Their results show that as the aspect ratio increases, separation and circulation occurs on the top surface of the cross section duct at fixed Rayleigh number and the corresponding behavior has observed through the isotherms. They have also obtained a general correlation using the aspect ratio as a parameter. Ali [13] has presented experimental study of natural convection heat transfer along square vertical ducts where laminar and transition modes are observed. Most recently, Correlations for horizontal triangular ducts in air are reported by Ali and Al-Ansary [14] where both laminar and transition regimes are discussed.

This paper presents the results of experimental investigations of laminar and transition to turbulence natural convection heat transfer from the outer surface of vertical ducts with triangular cross sections. The study focuses on the determination of axial (perimeter averaged) and overall averaged heat transfer coefficient in non-dimensional form of Nusselt numbers. Furthermore, general correlations using Nusselt numbers as function of the modified Rayleigh numbers are obtained for laminar and transition modes. General trends of laminar and transition regimes are discussed for different parameters.

2. EXPERIMENT SET-UP AND PROCEDURE

Figure 1 shows a schematic cross section view of the duct (D) and the thermocouple locations in

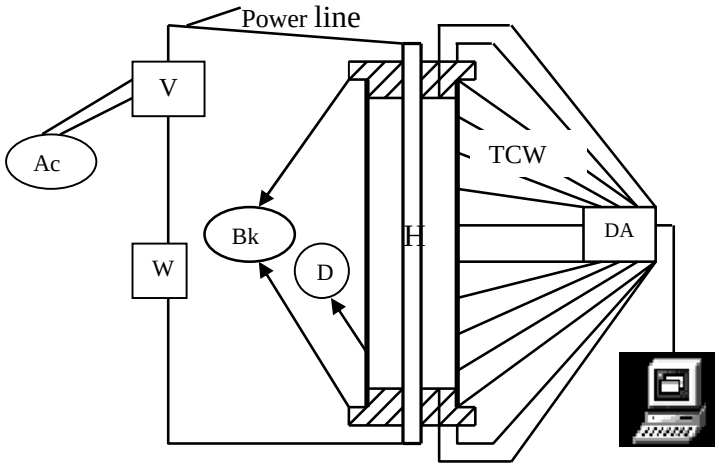

Figure 1. Schematic of the experimental system showing the thermocouple locations in the axial (TCW) direction

.

the vertical (axial) direction (TCW) on all sides of the duct. The ducts (D) were made from steel, hollow tube, (polished mild steel) with equilateral triangle cross sections of 0.044, 0.06 and 0,08 m, 1 m height and 0.002 m thick. An electrical heating element (H) (0.0066 m O.D.) was inserted into the center of the duct in order to heat the duct surface (D). Bakelite end plates (Bk, thermal conductivity = 0.15 W/mK [15]) 0.0206 m thick were attached at both ends of each test duct (D) to reduce the rate of axial conduction heat loss from the duct ends.

The surface temperature was measured at ten points in the vertical direction of each duct at the three vertical surfaces as seen in Fig. 1. Thirty two calibrated Nickel Chromium/Nickel Aluminium (type K) self adhesive thermocouples (0.3 second time response with flattened bead) were stuck on the duct surfaces 0.1 m apart and two of them were stuck on the outer surface of the Bakelite end plates; one at each plate. Two thermocouples ($0.01''$ or 0.25 mm dia. one at each plate) were inserted through the Bakelite thickness and leveled with its inside surface as seen in Fig. 1. The ambient air temperature was measured by one more thermocouple mounted in the room.

The duct was oriented vertically using a vertical stand in a room away from the openings of the ventilation and air conditioning system to minimize any possible forced convection. Those thermocouples were connected to forty channels data acquisition system (DA), which in turn were connected to a computer where the measured temperatures were stored for further analysis.

The input electrical power (Ac) to the heating element (H) was controlled by a voltage regulator (VR). The power consumed by the duct is measured by a Wattmeter (W) and assumed uniformly distributed along the duct length. The heat flux per unit surface area of the duct is calculated by dividing the consumed power (after deducting the heat loss by axial conduction through the Bakelite end plates and the radiation loss) over the duct outer surface area.

The input power to the duct increases for each duct from 4 to 480 W (corresponding to 13 V to 155 V) in two stages. In the first stage; the voltage increases in a step of 4 V up to a maximum of 36 V to observe any possible laminar natural convection regime. However, in the second stage it increases by 10 V, which presents the transition regime such that the maximum duct surface temperature does not exceed 160 ^{o}C. In other words, the experiment is done seventeen times for the larger cross section duct. Temperature measurements are taken after two hours of setting where the steady state should be reached. The procedure outlined above is used to generate natural convection heat transfer data in air (Prandtl number ≈ 0.71).

3. EXPERIMENTAL ANALYSES

The heat generated inside the duct wall dissipates from the duct surface by convection and radiation in addition to the heat lost by axial conduction through the Bakelite end plates.

$$Electrical\ input\ \ power = A_s\,(q_c + q_r) + A_{Bk}\,q_{Bk} \qquad (3)$$

Where q_c and q_r, are the fractions of the heat flux dissipate from the duct surface by convection and radiation, respectively. The heat flux lost by radiation (q_r) and by axial conduction through the Bakelite end plates (q_{Bk}) can be calculated respectively as:

$$q_r = \varepsilon\sigma\left(\overline{T}^4 - T_{surr}^4\right), \qquad q_{Bk} = k_{Bk}\,\frac{(T_{iB} - T_{oB})}{\delta} \qquad (4)$$

It should be noted that, q_r is estimated using the total overall averaged surface temperature $\overline{T}$ at each run of the duct and ε is the surface emissivity of the duct and it is estimated as 0.27 for polished mild steel [16]. Measurements show that, the

fraction of radiated heat transfer is 21 % of the total input power while the axial conduction heat lost through the Bakelite end plates is 3.5 % at most. Where, T_{iB} and T_{oB} are the measured inside and outside surface temperature of the Bakelite end plates, respectively and k_{Bk}, δ and T_{surr} present the Bakelite thermal conductivity, thickness, and the surrounding temperature respectively.

3.a Local vertical (perimeter averaged) heat transfer coefficient

In this case the perimeter averaged surface temperature at any distance x in the axial direction for each constant heat flux (run) is determined as:

$$T_x = \sum_{j=1}^{3} T_{xj} / 3, \tag{5}$$

where j is the number of thermocouples in the peripheral direction at any distance x along the vertical surface of the duct. The arithmetic mean surface temperature is calculated along the axial direction for each run as:

$$\theta_x = 0.5\left(T_x + T_\infty\right), \quad x = 1,2,\ldots..,10 \tag{6}$$

Therefore, for each heat flux (run) there are ten T_x axial temperature measurements. Consequently, once the electrical input power to the duct is measured, q_r and q_{Bk} from Eq. (4) and q_c from Eq. (3) then the axial (perimeter averaged) heat transfer coefficient h_x can be calculated from:

$$h_x = \frac{q_c}{T_x - T_\infty}, \qquad x = 1,2,3,\ldots,10 \tag{7}$$

Hence, the non-dimensional Nusselt and the modified Rayleigh numbers are obtained as

$$Nu_x = \frac{h_x x}{k}, \qquad Ra_x^* = \frac{g\beta q_c x^4}{\nu k \alpha} \tag{8}$$

All physical properties are evaluated at the axial perimeter averaged mean temperature θ_x for each q_c.

3.b Total overall averaged heat transfer coefficient

In this case the perimeter averaged heat transfer coefficient h_x is first evaluated at each distance x as in Eq. (7) and then the overall axial average $\bar{h}$ is obtained as:

$$\bar{h} = \sum_{x=1}^{10} h_x / 10 \tag{9}$$

Therefore, each heat flux q_c is presented by only one overall averaged heat transfer coefficient on contrary to the case (3.a) where q_c is presented by ten h_x's along the axial direction given by Eq. (7). All perimeter averaged physical properties are first obtained at θ_x then the overall averaged properties are obtained the same way following Eq. (9). The non-dimensional overall averaged Nusselt and the modified Rayleigh numbers are defined using the equilateral side length as a characteristic length L as:

$$\overline{Nu}_L = \frac{\bar{h} L}{k}, \qquad Ra_L^* = \frac{g\beta q_c L^4}{\nu k \alpha} \tag{10}$$

3.c Experimental uncertainty

In this section, the experimental uncertainty is to be estimated in the calculated results on the basis of the uncertainties in the primary measurements. It should be mentioned that, some of the experiments are repeated more than twice to check the calculated results and the general trends of the data especially in the laminar range of the experiment. The error in measuring the temperature, estimating the emissivity and in calculating the surface area is ± 0.2 ^oC, ± 0.02 and ± 0.003 m^2, respectively. The accuracy in measuring the voltage is taken from the manual of the Wattmeter as 0.5% of reading ±2 counts with a resolution of 0.1 V and the corresponding one for the current is 0.7% of reading ± 5 counts + 1 mA with a resolution of 1 mA.

At each run, forty scans of the temperature measurement are made by the data acquisition system for each channel and the mathematical average of these scans is obtained. Furthermore, since the input power, as mentioned earlier, has two stages; one for laminar and the other for transition then using the above mentioned errors turns to maximum itemized uncertainties of the calculated results shown in Table 1 for each range using the method recommended by Moffat [17]. Table 1 shows, in general, that the uncertainty of the quantities in the laminar regime is higher than that in transition regime which is expected since both the input power and the temperature range are very small.

Table 1. The maximum percentage uncertainties of various quantities in the laminar and transition regimes.

Quantity	Laminar	Transition
EIP	3.45	1.46
q_{Bk} up	6.14	4.89
q_{Bk} down	14.03	6.42
q_r	12.36	7.52
q_c	5.09	3.63
h_x	7.94	3.89
Nu_x	7.92	3.90
Ra_x^*	5.09	3.73
$\overline{Nu}_L$	5.60	3.05
$\bar{h}$	5.57	2.92
Ra_L^*	6.46	4.65

4. RESULTS AND DISCUSSIONS

Experimental data points are obtained for triangular ducts oriented vertically in air for heat flux rang 12 < q" < 1512 W/m^2 and for 24 < t_s < 160 ^oC. Within these parameter ranges the maximum local and average modified Rayleigh numbers are $1x10^{12}$ and $1x10^8$ respectively.

4(a)- Local heat Transfer results

Figure 2(a) shows the axial perimeter averaged surface temperature normalized by the ambient air temperature t_∞ as a function of the non-dimensional distance from the leading edge for several levels of heat fluxes q_c using duct number 1 (0.044 m). As seen in this figure, the temperature distribution increases as expected with the axial distance for uniform heat flux up to a critical value then it decreases. The region from the leading edge where a gradual increase in temperature occurs is characterized as laminar regime whereas transition occurs beyond the critical point similar to the case of vertical plate

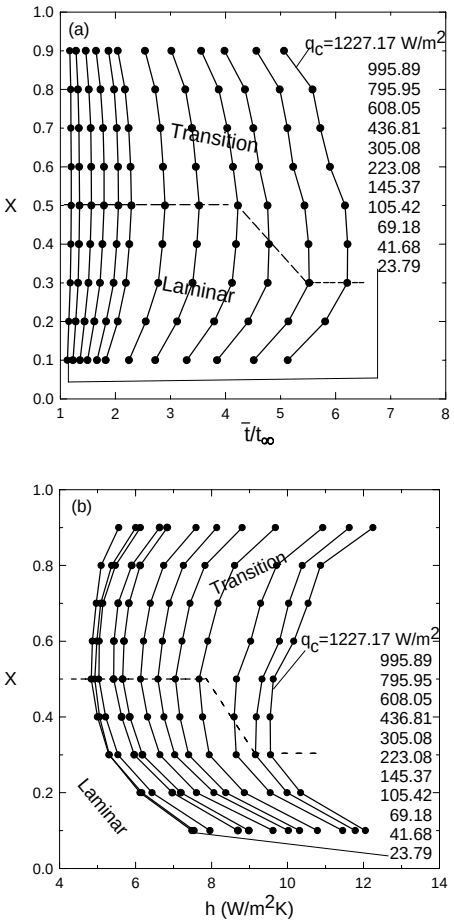

Figure 2. Axial perimeter averaged data along the duct surface for different levels of heat flux for duct number 1 (0.044 m); (a) dimensionless axial temperature distributions (b) the corresponding heat transfer coefficient.

(Vliet and Liu [1]). On the other hand, at any fixed distance from the leading edge the temperature increases as the heat flux increases. Figure 2(b) shows the profiles of the local (perimeter averaged) heat transfer coefficients corresponding to the same heat fluxes given in Fig. 2(a). As seen in this figure, two distinct regions can be classified; the region below the dashed line where the heat transfer coefficient decreases as the distance increases for fixed heat flux; therefore this region as mentioned earlier will be referred to as laminar. However, above the dashed line, heat transfer coefficient increases with the distance which means transition to turbulent occurs. It should be noted that duct number 2 (0.06 m) gives similar profiles for both temperature and heat transfer coefficient as for duct number 1. Figure 3(a) shows the temperature profiles along the normalized vertical distance for duct number 3 (0.08 m) at all levels of heat flux. As seen in this figure; the surface temperature increases all the way for low heat flux corresponding to laminar regime along the duct. Furthermore, as the heat flux

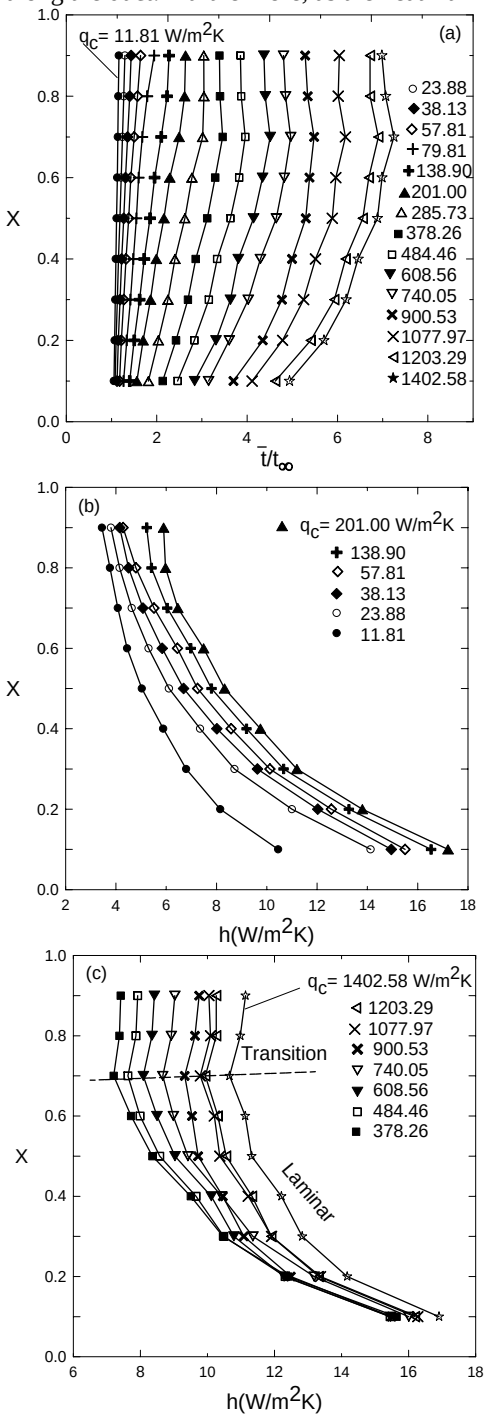

Figure 3. Axial perimeter averaged data along the duct surface for different levels of heat flux for duct number 3 (0.08 m); (a) dimensionless axial temperature distributions (b) the corresponding heat transfer coefficient showing the laminar range and (c) heat transfer coefficient with critical dashed line between the laminar and transition regions.

increases transition starts to appear as seen close to the upper end of the duct for $q_c \geq 378.26$ W/m^2. The corresponding local heat transfer coefficients are show in Fig. 3(b) for the same duct where laminar regime is dominated along the duct length with no transition regime. However, for $q_c \geq 378.26$ W/m^2 transition appears at x = 0.7 where heat transfer coefficient starts to increase as shown in Fig. 3(c). The dashed line in this figure separates two regions of interest; the first one below the line shows a reduction in heat transfer coefficient at fixed heat flux which will be called as before laminar whereas, above the dashed line the heat transfer coefficient starts to increase which presents the transition to turbulent regime near the top of the duct. The coordinates of the critical points where the transition begins are given in Table 2. Therefore, the transition to turbulent data is presented in a dimensionless form of the axial perimeter averaged Nusselt numbers and the modified Rayleigh numbers defined by Eq. (8) in Fig 4.

Table 2. Coordinates of critical (perimeter averaged) local axial points where transition begins.

Duct # 1 (0.044 m)			Duct # 2 (0.06 m)			Duct # 3 (0.08 m)		
X	h(W/m^{2}K), Nu_x	q″ (W/m^2), Ra^*_x	X	h (W/m^{2}K), Nu_x	q″ (W/m^2), Ra^*_x	X	h (W/m^{2}K), Nu_x	q″ (W/m^2), Ra^*_x
0.3	9.55, 93.21	1227.17, 1.30x10^{10}	0.4	10.51, 136.1	1512.78, 4.93x10^{10}	0.7	10.658, 243.62	1402.58, 4.55x10^{11}
	9.16, 91.28	995.89, 1.23x10^{10}		10.63, 140.02	1349.65, 4.96x10^{10}		9.94, 230.0	1203.75, 4.25x10^{11}
0.4	8.60, 116.21	795.95, 3.49x10^{10}		9.44, 125.34	1131.40, 4.39x10^{10}		9.79, 228.63	1077.97, 4.07x10^{11}
0.5	7.68, 131.55	607.22, 7.20x10^{10}		9.78, 132.83	968.24, 4.39x10^{10}		9.32, 221.0	900.53, 3.75x10^{11}
	7.05, 123.17	436.81, 5.90x10^{10}		9.29, 128.04	801.84, 4.03x10^{10}		8.67, 207.93	740.05, 3.36x10^{11}
	6.59, 117.23	305.08, 4.69x10^{10}		8.47, 118.12	644.66, 3.52x10^{10}		8.09, 196.19	608.56, 2.99x10^{11}
	6.13, 111.0	193.91, 3.35x10^{10}		7.99, 113.49	481.39x10^{10}		7.63, 187.53	484.46, 2.61x10^{11}
	5.66, 103.23	145.37, 2.65x10^{10}		6.49, 93.06	346.48, 2.29x10^{10}		7.20, 179.34	378.26, 2.23x10^{11}
	5.42, 99.59	105.42, 2.02x10^{10}		6.89, 100.61	254.27, 1.92x10^{10}	0.8	6.65, 191.66	285.73, 3.12x10^{11}
	5.03, 93.11	69.17, 1.39x10^{10}		5.65, 83.49	159.0, 1.30x10^{10}			
	4.93, 91.73	41.68, 8.78x10^{9}		5.36, 80.24	91.18, 8.18x10^{9}			
	4.83, 90.32	23.69, 5.11x10^{9}		6.31, 95.45	66.47, 6.37x10^{9}			
				6.08, 92.25	43.04, 4.22x10^{9}			
			0.5	5.60, 106.63	27.34, 6.72x10^{9}			
				4.64, 88.41	14.41, 3.59x10^{9}			

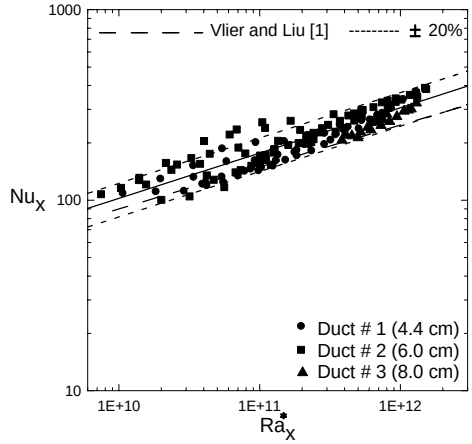

Figure 4. Local perimeter averaged Nusselt numbers vs. the modified Rayleigh numbers for the transition regime. Solid line present the data fit given by Eq. (11).

A least square power law fit through the data set (solid line) yields the following correlation:

$$\mathrm{Nu}_x = 0.426 \quad \left(\mathrm{Ra}_x^*\right)^{0.238}, 7.0\text{x}10^9 \le \mathrm{Ra}_x^* \le 2.0\text{x}10^{12} \qquad (11)$$

with correlation coefficient R = 92 %. The error bands of ± 20 % are also shown as dashed lines in the figure where only 13 points out of 143 are out of the bands or at the edge of the lines which means that 91 % of the data points lie inside the error bands. Comparison with the previously published data for turbulent natural convection over a vertical flat plate by Vliet and Liu [1] shows a fairly well agreement and it also shows that using the triangular ducts enhances the heat transfer coefficient over that of vertical plate.

As the laminar regime defined by the X-h plots (Figs. 2(b), 3(b), and 3(c)); Fig. 5 shows the local laminar regime covered by the three ducts. The correlation covering this data set is obtained as:

$$\mathrm{Nu}_x = 2.677 \quad \left(\mathrm{Ra}_x^*\right)^{0.160}, 4.0\text{x}10^6 \le \mathrm{Ra}_x^* \le 5.0\text{x}10^{11} \quad (12)$$

with correlation coefficient R = 92 %. Equation (12) indicates that the local heat transfer coefficient h_x decreases with the boundary layer length as $h_X \propto x^{-0.36}$ which ensures that (as shown earlier) the mode of heat transfer is absolutely laminar.

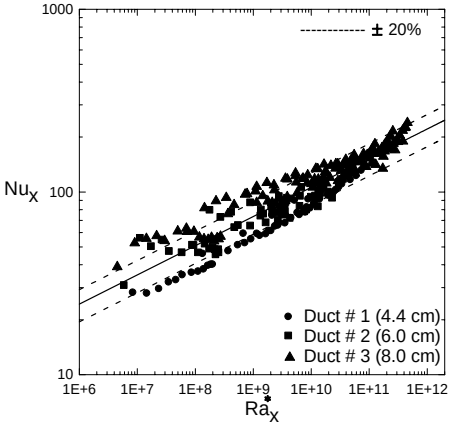

Figure 5. Local perimeter averaged data presenting laminar regime; Solid line present the data fit given by Eq. (12).

4(b)- Average heat Transfer results

The overall averaged results of the data are shown in Fig. 6 using all the ducts for all levels of heat fluxes. The correlation covering those data is given by:

$$\overline{\mathrm{Nu}}_L = 0.427 \quad \left(\mathrm{Ra}_L^*\right)^{0.230}, 4.0\text{x}10^5 \le \mathrm{Ra}_x^* \le 1.0\text{x}10^8 \qquad (13)$$

with a correlation coefficient R = 92.6 %. The error bands of ± 20 % are also shown as dashed lines in the figure where only 7 points out of 43 are out of the bands which means that 83.7 % of the data points lie inside the error bands.

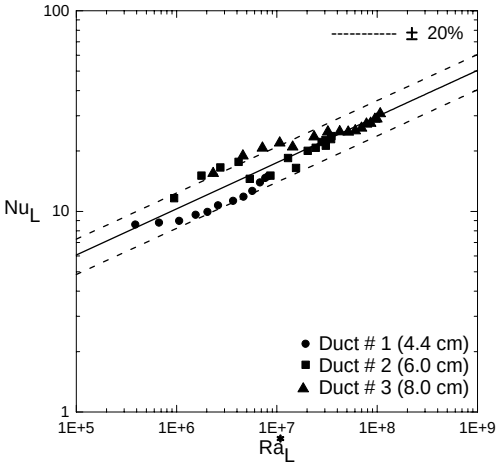

Figure 6. The overall averaged Nusselt numbers; solid line presents the fitting through the data given by Eq. (15).

Comparison with the results of Churchill and Chu [2] for turbulent natural convection from vertical plate is shown in Fig. 7 using the duct length H as a characteristic length, average surface temperature $\overline{T} = \sum_{x=1}^{11} T_x / 9$, and the average heat transfer coefficient $\overline{h}_1 = \frac{q_c}{\left(\overline{T} - T_\infty\right)}$ to be consistence with Eq. (2). The corresponding definitions of Nusselt and Rayleigh numbers are

$\overline{Nu}_H = \frac{\bar{h}_1 H}{k}$, and $Ra_H = \frac{g\beta(\bar{T} - T\infty)H^3}{\nu\alpha}$. This figure shows that using the triangular ducts enhances the heat transfer coefficient over the vertical plate approximation. Solid line presents the the correlation covering these data given by:

$$\overline{Nu}_H = 3.97 \quad (Ra_H)^{0.203}, \quad 2.0x10^8 \le Ra_x^* \le 6.0x10^9 \quad (14)$$

with a correlation coefficient R = 87.7 % and the dashed line presents Eq. (2) by Churchill and Chu [2].

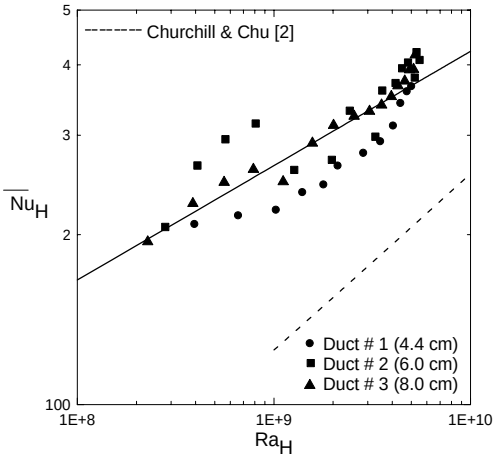

Figure 7. Comparison with Churchill and Chu [2] for turbulent natural convection from vertical plate using the duct height as a characteristic length.

5. CONCLUSIONS

Experimental study has been made on natural convection heat transfer from vertical triangular ducts in air. Two distinct flow regimes are observed; namely laminar and transition to turbulence. Laminar regime is obtained at the lower part of the ducts and is characterized by a decrease in the local axial (perimeter averaged) heat transfer coefficient along the duct height. However, transition to turbulent regime is characterized by an increase in the heat transfer coefficient at any fixed heat flux along the duct height. Two general correlations are obtained; one for laminar and the other for the transition regimes using the local axial Nusselt number and the modified Rayleigh number. Another overall averaged correlation is obtained using the averaged data and the equilateral triangular side length as a characteristic length. Furthermore, critical points where transition occurs are obtained and tabulated. Finally comparisons are made with the vertical plate correlations showing that using triangular ducts enhances the heat transfer coefficient.

Acknowledgments

This experimental investigation is supported by the Saudi Arabian Basic Industrial Company (SABIC) and the Research Center, College of Engineering at King Saud University under the project No. 6/429. This support is highly appreciated and acknowledged.

NOMENCLATURE

A	duct cross section length, m
A_c	duct cross section area, (A^2), m^2
A_s	duct surface area, (2A) l, m^2
A_{Bk}	end plate cross section area, m^2
B	duct cross section width, m
EIP	Electrical input power, W
H	duct height, m
h	heat transfer coefficient, W m^{-2} K^{-1}
k	thermal conductivity, W m^{-1} K^{-1}
L	equilateral side characteristic length, m
Nu	Nusselt number, h L / k or h x / k
q_c	convection heat flux, W/m^2
q_r	radiation heat flux, W/m^2
q_{Bk}	heat lost by conduction through the Bakelite end plates, W/m^2
Ra^*	the modified Rayleigh number, $g\beta q_c x^4 \nu^{-1}\alpha^{-1} k^{-1}$ or $g\beta q_c L^4 \nu^{-1}\alpha^{-1} k^{-1}$
T	temperature, K
T_{iB}	inside surface temperature of the Bakelite end plate
T_{oB}	outside surface temperature of the Bakelite end plate
t	temperature, ^oC
X	dimensionless axial distance, x/H
x	axial or axial distance, m

Greek symbols

α	thermal diffusivity, $m^2 s^{-1}$
β	coefficient for thermal expansion, K^{-1}
δ	Bakelite thickness
ε	emissivity
θ	arithmetic mean temperature defined by Eq. (6), K
ν	kinematics viscosity, $m^2 s^{-1}$
σ	Stefan- Boltzman constant, (= 5.67 x 10^{-8})

Subscripts

Bk	Bakelite
j	indices in the perimeter direction ranging from 1 to 3
L	characteristic length
x	indices in the axial direction ranging from 1 to 10
x	characteristic length
∞	ambient condition.

Superscripts

-	average quantity

REFERENCES

[1] Vliet, G. C. and Liu, C. K., 1969, "An Experimental Study of Turbulent Natural Convection Boundary Layers" Trans. ASME, J. of Heat Transfer, **91**(4), pp. 517-531.

[2] Churchill, S. W. and Chu, H. H., 1975, “Correlating Equations for Laminar and Turbulent Free Convection from a Vertical Plate,” Int. J. Heat Mass Transfer, **18**, pp. 1323-1329.

[3] Radziemska, E and Lewandowski, W. M., 2003, “Natural Convection Heat Transfer from Isothermal Cuboids” Int. J. Heat Mass Transfer, **45**, pp. 2169-2178.

[4] Kimura, F., Tachibana, T., Kitamura, K. and Hosokawa, T., 2004, “Fluid Flow and Heat Transfer of Natural Convection around Heated Vertical Cylinders” JSME International Journal, Series B, **47**(2), pp. 156-161.

[5] Gori, F., Serrano, M. G., and Wang Y., 2006, “Natural Convection along a Vertical Thin Cylinder with Uniform and Constant Wall Heat Flux” Int. J. of Thermophysics, **27**(5), pp. 1527-1538.

[6] Popiel, C. O., Wojtkowiak, J. and Bober, K., 2007, “Laminar Free Convection Heat Transfer from Isothermal Vertical Slender Cylinder” Experimental Thermal and Fluid Science, **32**, pp. 607-613.

[7] Ali, M. E., 1994, “Experimental Investigation of Natural Convection From Vertical Helical Coiled Tubes,” Int. J. Heat Mass Transfer, **37**(4), pp. 665-671.

[8] Ali, M. E., 1998, “Laminar Natural Convection From Constant Heat Flux Helical Coiled Tubes,” Int. J. Heat Mass Transfer, **41**(14), pp. 2175-2182.

[9] Ali, M. E., 2004, “Free Convection Heat Transfer From the Outer Surface of Vertically Oriented Helical Coils in Glycerol Water Solution," Heat and Mass Transfer, **40**(8), pp. 615-620.

[10] Ali M. E., 2006, "Natural Convection Heat Transfer From Vertical Helical Coils in Oil," Heat Transfer Engineering, **27**(3), pp. 79-85.

[11] Ali, M. E., 2007, "Natural Convection Heat Transfer from Horizontal Rectangular Ducts," ASME J. of Heat Transfer, **129**(9), pp. 1195- 1202.

[12] Zeitoun, O. and Ali, M., 2006, "Numerical Investigation of Natural Convection Around Isothermal Horizontal Rectangular Ducts," Numerical Heat Transfel, Part A, **50**, pp189 – 204, 2006.

[13] Ali, M. E., 2008, "Natural Convection Heat Transfer from Vertical Square Ducts" ASME 2008 Summer Heat Transfer Conference, August 10-14, Jacksonville, Fl., USA, ASME Paper # HT2008-56413.

[14] Ali, M. E. and H. Al-Ansary, 2009, "Experimental investigations on natural convection heat transfer around horizontal triangular ducts" Accepted for publication at Heat Transfer Engineering.

[15] William, D. and Callister, Jr., 2003, *Materials Science and Engineering An Introduction*, 6th ed, John Wiley & Sons, USA, Chap. 19. p. 660.

[16] Siegel, R. and Howell, J. R., 1992, Thermal Radiation Heat Transfer, 3rd edition, McGraw-Hill, New York.

[17] Moffat, R. J., 1988, “Describing uncertainties in experimental results”, Experimental Thermal and Fluid Science, **1**(1), pp. 3-7.